Structural relaxation and frequency-dependent specific heat in a supercooled liquid

Upendra Harbola and Shankar P. Das
School of Physical Sciences, Jawaharlal Nehru University, New Delhi 110067, India
(Received 22 March 2001; published 24 September 2001)

We have studied the relation between the structural relaxation and the frequency-dependent thermal response or the specific heat, $c_p(\omega)$, in a supercooled liquid. The mode coupling theory (MCT) results are used to obtain $c_p(\omega)$ corresponding to different wave vectors. Due to the two-step relaxation process present in the MCT, an extra peak, in addition to the low-frequency peak, is predicted in specific heat at high frequency.

DOI: 10.1103/PhysRevE.64.046122 PACS number(s): 64.70.Pf, 05.60.−k, 64.60.Cn, 47.35.+i

I. INTRODUCTION

Understanding the complex relaxation behavior in supercooled liquids has been a field of much research interest in recent times. In this regard the response of a system to an energy fluctuation, namely, the frequency dependence of specific heat of a supercooled liquid has been investigated by a number of authors. Generally, specific heat is a property that is usually linked to the thermodynamic property of a system. The pioneering experiments done by Birge and Nagel [1] have studied the dynamic response in glassy systems, namely, glycerol and propylene and obtained interesting dynamical response behavior, expressed in terms of a frequency-dependent specific heat [2]. In an experiment usually the frequency-dependent product of thermal conductivity (κ) and specific heat $\kappa c_p(\omega)$ is measured. However, in the temperature range 190–220 K, over which we are interested here, κ has weak frequency dependence [3,4] and hence the dynamics observed in the product $\kappa c_p(\omega)$ is entirely due to the frequency dependence of the specific heat. The theoretical modeling for the frequency dependence of specific heat in a supercooled liquid has been studied by various authors [5,6]. A new internal mode was proposed to be present in the supercooled liquid to explain the frequency-dependent response. In a simple analysis, Zwangig, however, had argued [7] that the frequency-dependence of the specific heat can be obtained without introducing any such internal mode. This work showed that what is measured as the frequency-dependent specific heat is actually related to that of the longitudinal viscosity in the liquid. In this model the dynamics of fluctuations around the equilibrium was studied in terms of a simple set of slow variables of hydrodynamics of fluids. These equations of motion used were the conservation laws of mass, momentum, and energy in the system. The resulting formula for the specific heat is equivalent to linking of the structural relaxation in a supercooled liquid to the frequency dependence of the specific heat. In the present work we take the data from the specific heat measurement [1] and extract the frequency dependence of the viscosity as will be required from such a formulation proposed in Ref. [7].

We then address the question if this value of the longitudinal viscosity will indeed be self consistent with independent measurements on the structural properties. The basic idea is to consider the frequency dependence of the specific heat solely in terms of the structural relaxation in the supercooled liquid.

For structural relaxation—the microscopic model for the liquid dynamics, namely, the mode coupling theory (MCT) has been studied by a number of authors in recent years [8,9]. A simple application [2] of the MCT to fit the specific heat data indicated that a very large exponent is required to match the experimental data to power law divergence. In the present work we also use the MCT as a model for structural relaxation and obtain the corresponding frequency dependence of the longitudinal viscosity. We then use it to predict the behavior of the specific heat with frequency as predicted from the theory proposed in Ref. [7]. In the microscopic model of the mode coupling theory the wave number dependence of the longitudinal viscosity is obtained using proper input for the structure factor of the liquid. For this purpose standard results from the integral equations for simple liquids are used for the structure factor. The frequency-dependent specific heat is then computed for different wave numbers. Thus, the effect of the response to heat fluctuations can be computed over different length and time scales in the present approach. While this extends the theory with scope of further comparison, the main goal of the present work is to test if the frequency dependence of the specific heat can be understood solely in terms of the structural relaxation and if the two sets of measurements agree in a self-consistent manner. The paper is organized as follows. In the following section, Sec. II, we consider the schematic model for the time dependence of the viscosity and in Sec. III, we compare the theoretical results with the experimental observations. A wave number dependent calculation for the specific heat is presented in Sec. VI. In Sec. V, we present the mode coupling results for the specific heat over different length scales and temperatures. In the last section we discuss the results.

II. FREQUENCY-DEPENDENT SPECIFIC HEAT

Since we are concerned here with the dynamic properties of a supercooled liquid, an obvious choice is to consider a hydrodynamic model for the system. To start with, we write down the linearized hydrodynamic equations

$$\frac{\partial}{\partial t}\delta\rho + \vec{\nabla}\cdot\vec{g} = 0, \tag{1}$$

$$\frac{\partial g_i}{\partial t}+\nabla_i P-\eta\nabla^2\vec{g}_i-\left(\frac{1}{3}\eta+\zeta\right)\nabla_i(\vec{\nabla}\cdot\vec{g})=0, \tag{2}$$

$$\rho_o c_v\frac{\partial}{\partial t}\delta T+\kappa\nabla^2 T+\frac{T_o}{\rho_o}\left(\frac{\partial P}{\partial T}\right)_\rho\vec{\nabla}\cdot\vec{g}=0, \tag{3}$$

governing the time evolution of fluctuations of conserved variables mass density (ρ), momentum density ($\vec{g}$), and the temperature (energy) T. Here ρ_o and T_o represent equilibrium density and temperature, respectively, and $\delta\rho$ and δT are the fluctuations from the equilibrium values. c_v is the specific heat per unit mass at constant volume and η and ζ are the shear and bulk viscosities, respectively. The viscosity coefficients here are divided by the density. The fluctuation of the pressure P around the equilibrium value can be expanded to the lowest order in density and temperature as

$$\delta P=\left(\frac{\partial P}{\partial\rho}\right)_T\delta\rho+\left(\frac{\partial P}{\partial T}\right)_\rho\delta T, \tag{4}$$

where we have assumed that the change of the pressure functional with the density function at the equilibrium can be replaced by the equilibrium partial derivative — replaced by the corresponding thermodynamic quantity. Using the above equations the energy conservation equation (3) reduces to the Fourier heat law for thermal fluctuations,

$$\iota\omega\,\delta T=\mu(\omega)\nabla^2\delta T, \tag{5}$$

with the frequency-dependent thermal diffusivity $\mu(\omega)$ defined in terms of the specific heat c_p as

$$\mu(\omega)=\frac{\kappa}{\rho_o c_p(\omega)}. \tag{6}$$

The specific heat $c_p(\omega)$ is expressed in the form

$$c_p(\omega)=c_v+(c_p-c_v)\frac{K_T(0)}{K_T(\omega)}. \tag{7}$$

The quantity $K_T(\omega)$ is called the generalized bulk modulus and is given by

$$\frac{K_T(\omega)}{K_0}=1+\iota\omega\Gamma(\omega) \tag{8}$$

and is expressed in terms of the reduced form $\Gamma(\omega)=\eta_l(\omega)/c_o^2$ of the frequency-dependent longitudinal viscosity $\eta_l(\omega)$. In equation (8), K_0 is the $\omega=0$ limit of $K_T(\omega)$. Obviously for the liquid state with finite viscosity the zero frequency limit of $K_T(\omega)$ relates to the thermodynamic property of the supercooled liquid. The sound speed c_o is given by

$$c_o^2=\left(\frac{\delta P}{\delta\rho}\right)_T=\frac{K_0}{\rho_o}. \tag{9}$$

A frequency-dependent longitudinal modulus $M(\omega)$, the inverse of compliance, is defined along a similar line as

$$\frac{M(\omega)}{K_0}=\gamma+\iota\omega\Gamma(\omega), \tag{10}$$

where γ is the ratio of the long time limit of the specific heat $c_p(\omega=0)$ to c_v. Equation (7) is the key formula used in this paper for testing the idea of modeling the frequency dependence in the specific heat solely in terms of the structural relaxation. In obtaining equation (5), one also needs to assume that the following self-consistent relation holds:

$$\Delta(\omega)\equiv(\gamma-1)\frac{\omega}{\bar{M}(\omega)[\omega+i\nu\bar{M}(\omega)]}\ll 1. \tag{11}$$

Here we have expressed M in the dimensionless form as $\bar{M}(\omega)=M(\omega)/K_0$. $\nu=c_0^2/\mu_o$, with $\mu_o=\kappa/(\rho_o c_v)$ is the bare thermal diffusivity. We test the validity of the assumption (11) in the frequency range where the analysis with respect to experimental data is made.

III. COMPARISON OF EXPERIMENTAL DATA

In this section we test the self-consistency in expressing the frequency-dependent data on specific heat and structural relaxation. For the supercooled liquids the relaxation over longest time scales, i.e. the α relaxations, follows the stretched exponential behavior

$$\eta(t)=\eta_o\exp\left[-\left(\frac{t}{\tau}\right)^\beta\right], \tag{12}$$

where η_o is the amplitude and β is the stretching parameter that defines the degree of deviation from the exponential decay. In fitting the specific heat data we use the dimensionless form for the specific heat ratio

$$c_p(\omega)=c_v\left[1+\frac{(\gamma-1)}{1+\iota\omega\Gamma(\omega)}\right], \tag{13}$$

which reduces the formula in a dimensionless form. We fit the specific heat data of Ref. [1] to the formula (13) using a simple stretched exponential (12) relaxation function. In Figs. 1(a) and 1(b) we show the respective fitting of the experimental data for the real and imaginary parts of $c_p(\omega)$ in the supercooled glycerol for three different temperatures, $T=201.4$ K, 203.9 K, and 211.4 K. The points marked with dots, circles, and squares correspond to the experimental data of Refs. [1,20] for supercooled glycerol. The arrows in Fig. 1(b) indicate the peak positions in the imaginary parts of the viscosities at the corresponding temperatures. In calculating the specific heat, the three parameters $\Gamma(t=0)$, the relaxation time τ and the stretching exponent β are used as the free parameters and $\gamma=1.86$. Using the best fit values of the parameters with the specific heat data we compute the structural properties of the liquid given by modulus $M(\omega)$ defined in Eq. (10) and the longitudinal viscosity. The resulting behaviors for these quantities are compared with the experimental results as shown in Figs. 2 and 3.

In Fig. 2, we show the viscosity η in the zero frequency limit in units of $K_o\tau_o$ where τ_o is the unit of time used. In the

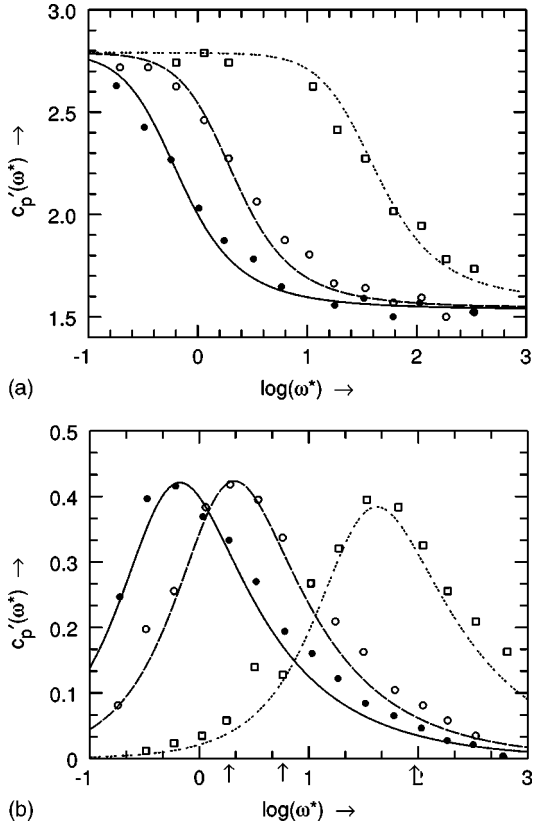

FIG. 1. (a) Continuous lines show the theory fit to the experimental data (dots, square and circles) of Refs. [1,20] for the real part $c_p'(\omega)$ of the specific heat $[c_p(\omega)]$ of supercooled glycerol at three temperatures $T=201.4$ K (continuous line), 203.9 K (long dashed) and 211.4 K (dotted). $\omega^*=\omega\tau_o$, where τ_o is the units of time used (see text). (b) Imaginary parts $c_p''(\omega)$ of specific heat corresponding to the real parts shown in (a). Theoretical values are plotted as continuous lines. Dots, squares, and circles are the experimental data of Refs. [1,20]. Arrows along the frequency axis indicate the peak position in the imaginary part of the corresponding viscosity.

inset we show the corresponding experimental data [10,11] for the viscosity. The experimental data shown here is over a much wider temperature range (317–190 K) — both theoretical and experimental data agree with the Vogel-Fulcher (VF) fit ($\eta\sim\exp[A/(T-T_o)]$ for $T_o=128$ K and $A=2559$ K shown in both the figure and the inset as solid lines. The zero frequency modulus K_o is roughly temperature independent [12] over the range considered here. We notice that the viscosity increases by four orders of magnitude as the temperature is decreased over a small range (200–220 K) near the glass transition temperature ($T_g=190$ K) [13].

We define a normalized longitudinal modulus

$$\tilde{M}(\omega)=\frac{M(\omega)-M(0)}{M(\infty)-M(0)}. \tag{14}$$

In Figs. 3(a) and 3(b) we show the real and imaginary parts of $\tilde{M}$, respectively, denoted by $M'(\omega)$ and imaginary $M''(\omega)$ against the frequency for the three different temperatures, $T=203.9$ K (solid), 211.4 K (dashed), and 221.5 K

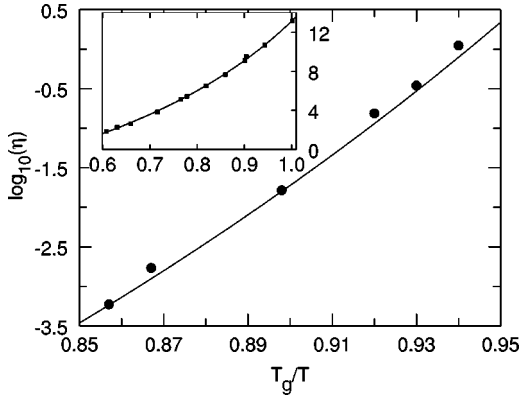

FIG. 2. Temperature variation of viscosity in supercooled glycerol as obtained from the specific heat fitting. Viscosity is given in units of $K_o\tau_o$. Experimental results for the viscosity are shown in the inset. The continuous line (both in the main figure and the inset) is the Vogal-Fulcher fit, $\eta=\eta_o\exp[A/(T-T_o)]$, with $A=2559$ K and $T_o=128$ K. T_g is the glass transition temperature for the glycerol (see Ref. [13]).

(dotted) lines. The frequency in each case is expressed in terms of the ratio with the corresponding peak position ω_p in the imaginary part. The corresponding results from measurements on the modulus $\tilde{M}$ [14] are also shown with filled circles. In Fig. 4 we show the plot of the peak positions as found in the fitting of the specific heat curves with different temperatures. As the temperature is decreased, peak in the imaginary part of the specific heat shifts towards the lower temperatures, signifying the slower relaxations in the system. The solid line indicates VF fit with $T_o=128$ K. In Fig. 5, we show the frequency-dependent specific heat and the viscosity function (in the inset) at the same temperature. The peaks appear nearly at the same position on the frequency scale for the two quantities showing that the dominant time scales are same in the two cases. Finally we test the validity of the assumption (11) that is crucial in reaching the Fourier heat law (5) with the frequency-dependent specific heat — defined above. For this we calculate both the real $[\Delta'(\omega)]$ and the imaginary $[\Delta''(\omega)]$ parts of $[\Delta(\omega)]$ for the supercooled glycerol. In Fig. 6 we plot both the real and the imaginary parts of $\Delta(\omega)$ on the frequency range over which specific heat (frequency dependent) is observed. These figures clearly show that the quantity $\Delta(\omega)$ is much smaller as compared to unity over this frequency range. This substantiates the assumption made in the preceding section to reach the Fourier heat law in a generalized sense.

IV. WAVE VECTOR DEPENDENCE OF SPECIFIC HEAT

In the preceding section, we studied the specific heat and other quantities like longitudinal viscosity and modulus using a schematic model to show the self-consistency of the relation between structural relaxation and the frequency dependence of specific heat. Here we consider the wave vector and frequency-dependent specific heat in a liquid. Starting from the generalized hydrodynamic equations for the conserved densities in q space, we obtain an equation,

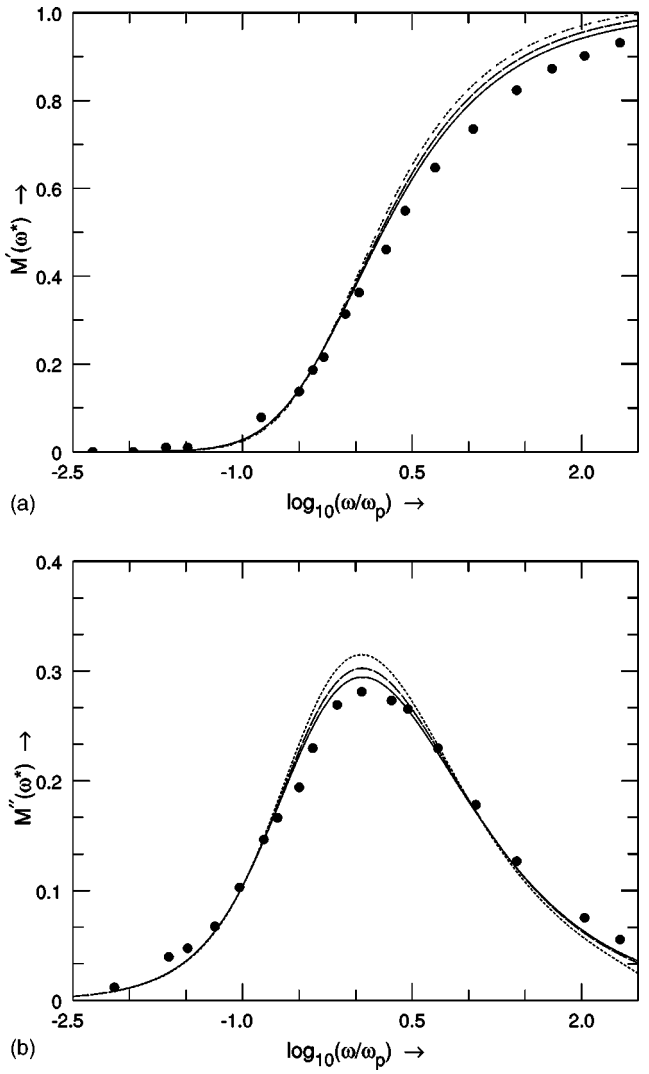

FIG. 3. (a) Real part $M'(\omega)$ of the normalized longitudinal modulus $\tilde{M}(\omega)$ (see text) is plotted at three different temperatures $T=203.9$ K (solid line), 211.4 K (dashed line), and 221.5 K (dotted line). Dots are the experimental results of Ref. [14]. Frequency axis is scaled with respect to the peak values ω_p for the three different temperatures and $\omega^*=\omega\tau_o$. (b) Imaginary parts of the normalized longitudinal modulus $\tilde{M}(\omega)$ corresponding to the real parts shown in (a). Dots are the experimental results of Ref. [14]. $\omega^*=\omega\tau_o$.

$$\iota\omega\rho_o c_v \delta T(q,\omega) = -q^2\kappa\delta T(q,\omega) + \frac{\iota q^2\omega T_o}{\rho_o\omega^2 - q^2 K_T(q,\omega)}\left(\frac{\partial P}{\partial T}\right)_\rho^2 \delta T(q,\omega) \tag{15}$$

that describes dynamics of the energy fluctuations over different length and time scales. $K_T(q,\omega)$ is the wave vector and frequency-dependent bulk modulus given by

$$\frac{K_T(q,\omega)}{K_T(q)} = 1 + \iota\omega\Gamma(q,\omega), \tag{16}$$

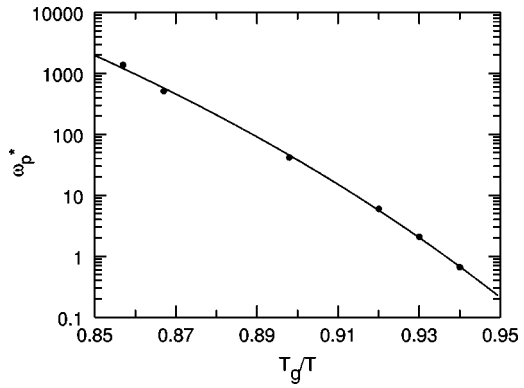

FIG. 4. Peak position ω_p in the imaginary part of the specific heat is plotted as a function of the temperature T. Continuous line is the VF fit: $\omega_p=\omega_o\exp[-A/(T-T_o)]$; with $\omega_o=1.0\times10^{15}$ Hz, $A=2559$ K and $T_o=128$ K. T_g is same as in Fig. 2. ω_p^* is the peak frequency in the units of $1/\tau_o$.

where $\Gamma(q,\omega)$ is the wave vector and frequency-dependent longitudinal viscosity divided by the square of the speed of sound $c_s^2(q)=K_T(q)/\rho_o$. $K_T(q)$ is the zero frequency limit of $K_T(q,\omega)$. The energy equation (15) reduces to the wave vector dependent Fourier heat equation

$$\iota\omega\delta T(q,\omega) = -q^2\chi(q,\omega)\delta T(q,\omega) \tag{17}$$

where $\chi(q,\omega)=\kappa/[\rho_o c_p(q,\omega)]$ is thermal diffusivity and $c_p(q,\omega)$ is the q-dependent specific heat given by

$$c_p(q,\omega) = c_v\left[1+(\gamma_q-1)\frac{1}{1+\iota\omega\Gamma(q,\omega)}\right] \tag{18}$$

and γ_q is the ratio $c_p(q)/c_v$. Here in obtaining the Fourier heat equation (17), we have assumed that the quantity

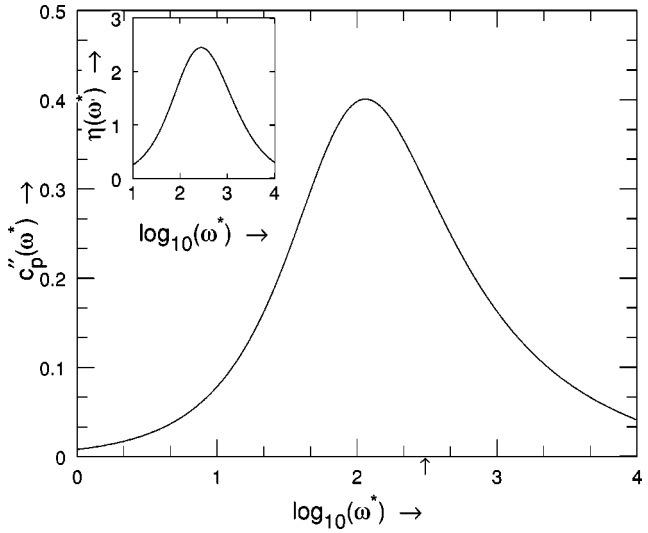

FIG. 5. Imaginary part of the specific heat $c_p''(\omega)$ at $T=214$ K. Arrow along the frequency axis at 2.45 indicates the peak position in the imaginary part of the corresponding viscosity shown in the inset.

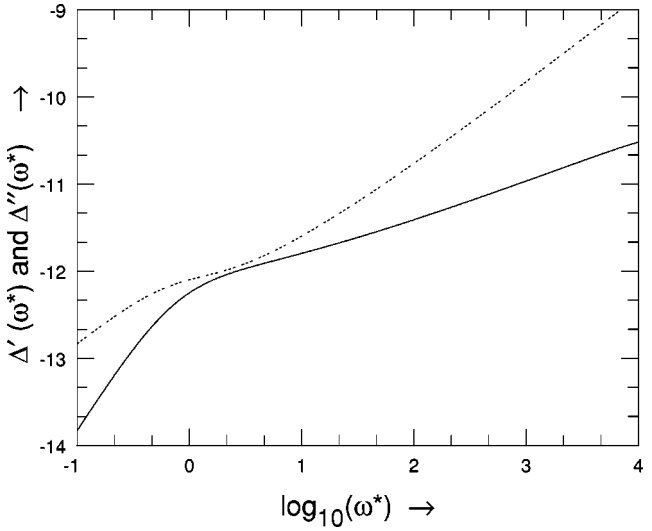

FIG. 6. Log (base 10) of the real (continuous curve) and imaginary parts (dotted curve) of $\Delta(\omega)$(see text), for supercooled glycerol, are plotted with frequency at $T=201.4$ K. $\omega^*=\omega\tau$.

$$(\gamma_q-1)\frac{\omega}{\bar{M}(q,\omega)[\omega+\iota\nu(q)\bar{M}(q,\omega)}\ll 1, \qquad (19)$$

where $\nu(q)=c_s^2(q)/\mu_o$ and $\bar{M}(q,\omega)=\gamma(q)+\iota\omega\Gamma(q,\omega)$, is much smaller as compared to unity. In the long wavelength limit, this quantity reduces to $\Delta(\omega)$ given by Eq. (11).

V. RESULTS FROM THE MODE COUPLING THEORY

In this section, we consider the time-dependent longitudinal viscosity obtained from a microscopic theory of statistical mechanics, instead of taking inputs from experimental results as was done in the Sec. III. We predict structural aspects, i.e., the wave vector dependence in the specific heat at different frequencies.

In the simplest form the self-consistent mode coupling theory predicts a sharp transition of the supercooled liquid to nonergodic phase. The temperature at which this transition takes place is known as the critical temperature T_c. In later versions, however, it was shown that due to coupling of density fluctuations with currents this sharp transition is eliminated — the full model with the cutoff mechanism included is termed as the extended model. In this work we consider the extended model where the cutoff function is adjusted to obtain agreement with the viscosity of the supercooled liquid to the results obtained from computer simulations. The details of the model and the scheme for computation of the density correlation function using the proper cutoff function is presented elsewhere [15]. We consider a one-component Lennard-Jones (LJ) system for computing the structural relaxation properties using the MCT. The temperature T^* and density ρ^* are expressed in the standard units of ϵ/K_B and σ^3, respectively. ϵ is the unit of energy in a LJ system and σ is the diameter of a particle. For the system considered here (LJ), T_c (in units of ϵ/K_B) is around 0.93. In computing the dynamical behavior of the density correlation function we

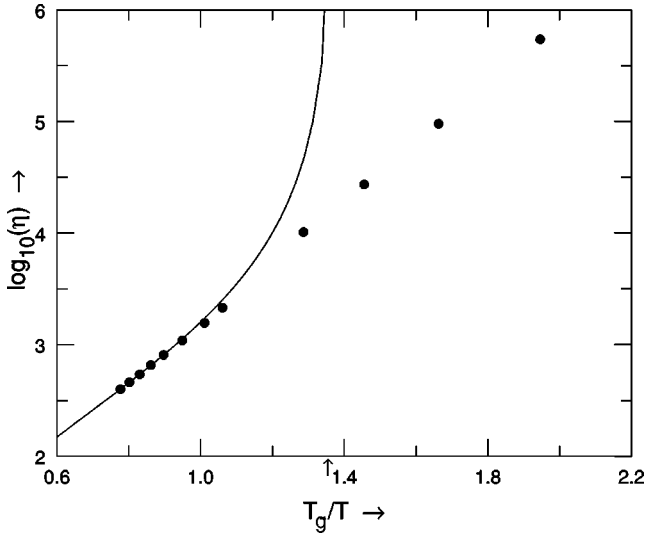

FIG. 7. Mode coupling viscosity [in units of $(1/\beta\sigma^2)\sqrt{m/\epsilon}$] is plotted as a function of temperature. For temperatures ($T>T_c$) it follows a power law behavior (shown as a continuous line) with exponent 1.9. Arrow along the temperature axis at $T_C/T=1.36$ indicates the power law divergence as predicted by the simplified version of the MCT. Temperature is in the units of ϵ/K_B.

estimate the cutoff parameters of the theory so that the shear viscosity obtained from the self consistent MCT [15] agrees with the computer simulation results. For the simulation results on one-component model we use the recent results of Ruocco and coworkers [16] using special techniques that avoid the typical problem of crystallization in one-component systems. From the self-consistent results for the density correlation functions we compute the mode coupling integrals for the longitudinal part of the memory function related to the decay of the density correlation functions.

The longitudinal viscosity in the zero wave number limit is shown in Fig. 7 (with dots) for the temperature range around T_c. The longitudinal viscosity shown for the temperature range around T_c/T less than 1, follows the power law behavior as shown in the figure with continuous line. For temperatures higher than T_c, viscosity diverges with power law exponent equal to 1.9 and for lower temperatures ($T_c/T>1$) the behavior follows a Vogel-Fulcher form (not shown) with VF parameter $T_o=0.023$. This is usual with results of the extended MCT [17]. We then use this frequency-dependent memory function or the longitudinal viscosity to compute the corresponding frequency-dependent specific heat. In the mode coupling approximation, the normalized longitudinal viscosity $\Gamma(q,\omega)$ is given by

$$\Gamma(q,\omega)=\frac{1}{2n}S(q)\int dt e^{\iota\omega t}\int\frac{d\vec{k}}{(2\pi)^3}\left[\frac{\hat{q}\cdot\vec{k}}{q}c(k)+\frac{\hat{q}\cdot(\vec{q}-\vec{k})}{q}c(|\vec{q}-\vec{k}|)\right]^2\psi(k,t)\psi(|\vec{q}-\vec{k},t), \qquad (20)$$

where $\psi(q,t)$ and $S(q)$ represent density correlation function and the structure factor, respectively. $c(q)$ is the direct

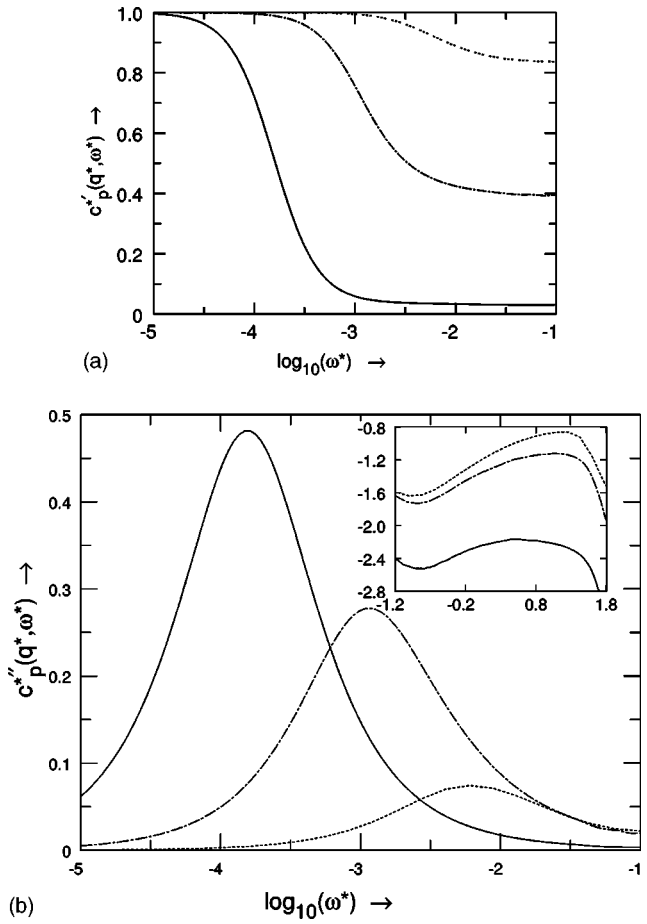

FIG. 8. (a) MCT results for the real part of the normalized specific heat $c_p^*(q,\omega)=[c_p(q,\omega)-c_v]/[c_p(q)-c_v]$ for three wave vectors $q^*=0$ (dotted), 7.05 (continuous), and 30 (dashed) at $T^*=0.559$. Here frequency ω^* is in the units of the inverse of Lenard-Jones time, $\tau=\sqrt{m\sigma^2/\epsilon}$. (b) Imaginary part of $\tilde{c}_p(q,\omega)$ from the MCT corresponding to the real parts shown in (a). Inset shows the secondary peaks predicted by the MCT for the same three q values.

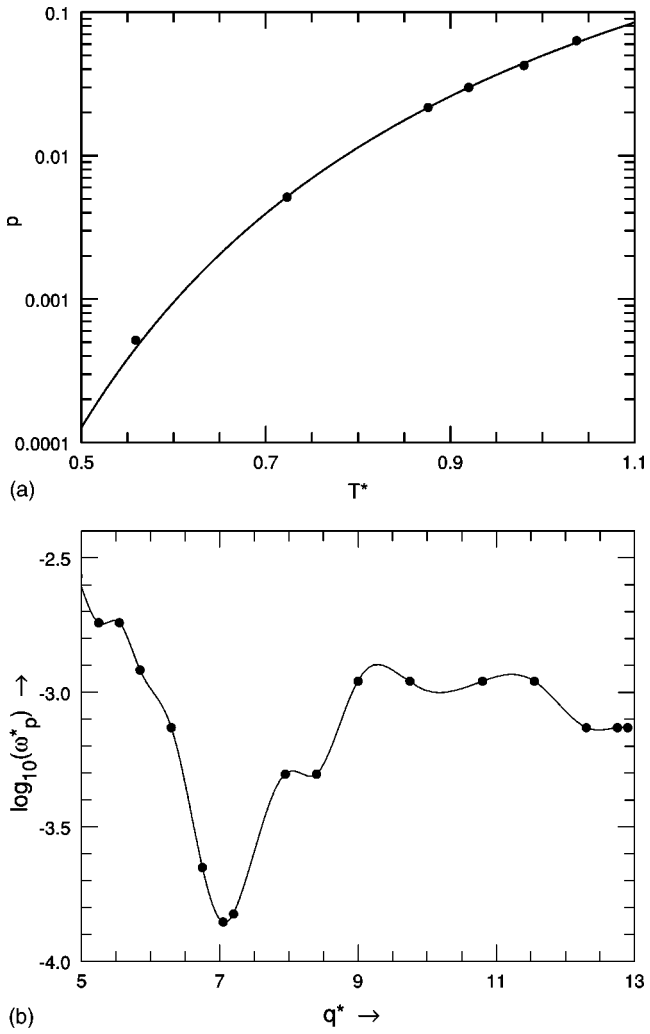

FIG. 9. (a) Variation of the peak position ω_p in the specific heat $\tilde{c}_p(q,\omega)$ with temperature for $q=0$. T^* is in the units of ϵ/K_B. along the vertical axis, we have shown $\omega_p^*=\omega\tau\times 10^2$. (b) Variation of the peak frequency ω_p with wave vector q^*. ω_p reaches to minimum at $q^*=7.05$ at which the structure factor shows a maximum. $\omega_p^*=\omega\tau\times 10^2$. Solid line is a smooth fit to the calculated values of ω_p (shown with dots) at different wave vectors q^*.

correlation function of the system. $\hat{q}$ denotes the unit vector along $\vec{q}$ and n is the number density. Using the above expression for the longitudinal viscosity in Eq. (18), we calculate the q-dependent specific heat in the supercooled liquid. The only input required in calculating the longitudinal viscosity is the structure factor of the system.

In Figs. 8(a) and 8(b) we show, respectively, the real and imaginary part of $c_p^*(q,\omega)$ vs the frequency. This is shown here for three different wave vectors, $q^*=0$, 7.05 (peak of the structure factor), and 30 (upper cutoff taken for the k integral) at temperature $T^*=0.559$. Here q^* is the wave vector expressed in the units of σ. The insets of the corresponding figures show the secondary peak predicted for fast processes at very high frequency window — representing the so called β processes in the supercooled liquid. The peak in the imaginary part shifts to lower frequency with lowering of temperature. In Fig. 9(a) we show the variation of the peak position with temperature of the liquid. The solid line in the figure shows Vogel-Fulcher fit with $T_o=0.014$. This T_o value is different from the one obtained by fitting the viscosity data as mentioned above. The slight difference in the two T_o values is due to the fact that the viscosity follows the Vogel-Fulcher behavior over a smaller temperature range ($T<T_c$) while the peak frequency fits it over the entire temperature range considered here. In order to indicate the structural dependence we also show in Fig. 9(b), the dependence of the peak position on the wave number q at a fixed temperature $T^*=0.559$. The peak frequency signifying the dominant time scale for relaxation at different wave numbers follows the nature of the structure factor. It shows a minimum at q value that corresponds to the peak in the structure factor of the liquid. Successive minima in the figure correspond to the other less pronounced maxima in the structure factor.

VI. DISCUSSION

In Sec. III, we considered two types of experimental measurements on the supercooled liquids, respectively, related to the energy fluctuations and the structural relaxations. This was done to check the consistency of the formula for specific heat obtained from simple analysis of the hydrodynamic equations. The comparisons done in Sec. III indicate that the frequency-dependent specific heat can be understood in terms of the structural relaxation data in terms of the analysis proposed in Ref. [7].

Subsequently we apply the standard forms of the self-consistent mode coupling theory to compute the frequency dependence of the viscosity and compute those for the specific heat in a supercooled LJ system. Here we use the formula in terms of the generalized hydrodynamics, extending the model to large k, or small wavelengths. We find that the dispersion in the specific heat decreases as we go to the smaller length scales (higher q^*) with corresponding increase in spectrum width. This demonstrates the fact that at short length scales the relaxation is fast and here the memory effects reflecting cooperativeness are not strong.

The peak position ω_p in the imaginary part of the $c_p^*(q,\omega)$ shifts to higher frequency with the increase of the corresponding wave vector q^*. It however reaches to a minimum frequency at the structure factor peak. Finally, since the MCT relates to the two-step relaxation process in supercooled liquids, there is a corresponding implication on the specific heat curve predicting a peak at very high frequency in the specific heat. This is shown in the inset of Fig. 8(b). It is a consequence of secondary relaxation in the supercooled liquid. Due to the constraints on the MCT at very low temperatures, we could not study the thermal response of the system close to the glass transition temperature T_g. However, as is shown in the Fig. 9(a), the main peak in the specific heat moves towards the smaller frequencies with decreasing temperature, thus at the temperatures very close to the glass transition one can expect the two peaks to lie further apart from each other.

We have ignored here effects of nonlinearities in the energy equation [18,19]. This can produce frequency dependence on other transport coefficients like thermal conductivity as well. However, observation of such a peak will further strengthen the validity of the simple analysis presented here in energy transport in terms of structural relaxation behavior.

ACKNOWLEDGMENTS

We are grateful to Professor N. O. Berge for providing data on specific heat measurements. U.H. acknowledges the financial support from the University Grant Commission, India. The authors thank the Hahn Meitner Institute, Berlin, Germany for providing computational facilities.

[1] N.O. Birge and S.R. Nagel, Phys. Rev. Lett. **54**, 2674 (1985).
[2] M.C. Marchetti, Phys. Rev. A **33**, 3363 (1986).
[3] D.G. Cahill and R.O. Pohl, Phys. Rev. B **35**, 4067 (1986).
[4] P.K. Dixon and S.R. Nagel, Phys. Rev. Lett. **61**, 341 (1988).
[5] D.W. Oxtoby, J. Chem. Phys. **85**, 1549 (1986).
[6] J.K. Nielsen and J.C. Dyre, Phys. Rev. B **54**, 15 754 (1996).
[7] R. Zwanzig, J. Chem. Phys. **88**, 5831 (1988).
[8] W. Götze, in *Liquids, Freezing and the Glass Transition,* edited by D. Levisque, J.P. Hansen, and J. Zinn-Justin (Elsevier, New York, 1991).
[9] B. Kim and G.F. Mazenko, Adv. Chem. Phys. **78**, 129 (1990).
[10] C.A. Angell, J. Non-Cryst. Solids **102**, 205 (1988).
[11] G. Tarjus and D. Kivelson, e-print cond-mat/0003368.
[12] R. Meister, C.J. Marhoeffer, R. Sciamanda, L. Cotter, and T. Litovitz, J. Appl. Phys. **31**, 854 (1960).
[13] R. Böhmer, K.L. Ngai, C.A. Angell, and D.J. Plazek, J. Chem. Phys. **99**, 4201 (1993).
[14] Y.H. Jeong, S.R. Nagel, and S. Bhattacharya, Phys. Rev. A **34**, 602 (1986).
[15] S. Srivastava and S.P. Das (unpublished).
[16] L. Angelani, G. Parisi, G. Ruocco, and G. Viliani, Phys. Rev. Lett. **81**, 4648 (1998).
[17] S.P. Das, Phys. Rev. A **42**, 6116 (1990).
[18] B. Kim and G.F. Mazenko, J. Stat. Phys. **64**, 631 (1991).
[19] D.N. Zuberev and V.G. Morozov, Physica A **120**, 411 (1983); V.G. Morozov, *ibid.* **126**, 443 (1984).
[20] N.O. Birge (Private communication).